X-RAY EMISSION LINE GAS IN M81

M. J. Page [a] R. Soria [a] K. Wu [a] A. A. Breeveld [a] G. Branduardi-Raymont [a] K. O. Mason [a] R. L. C. Starling [a] S. Zane [a]

[a]Mullard Space Science Laboratory, Holmbury St Mary, Dorking, Surrey RH5 6NT, UK

The soft X-ray spectrum of the LINER galaxy M81, from a long observation with the *XMM-Newton* RGS, contains emission lines from Fe-L, H-like and He-like N, O, and Ne. The emission lines are significantly broader than the RGS line spread function and are found adjacent to as well as coincident with the active nucleus. This implies that they originate in a region of a few arcminutes (kpc) extent. The flux ratios of the O VII triplet suggest that the gas is collisionally ionized. A good fit to the whole RGS spectrum can be obtained with an absorbed power law from the active nucleus and a 3-temperature optically thin thermal plasma. Two of the thermal plasma components have temperatures of 0.18 ± 0.04 and 0.64 ± 0.04 keV, consistent with a hot interstellar medium produced by supernovae. The third thermal plasma component has a higher temperature ($1.7^{+2.1}_{-0.5}$ keV); we argue that this emission is likely to come from low-mass X-ray binaries in the bulge of M81.

1. Introduction

M81 is an Sab spiral galaxy hosting a low luminosity Seyfert nucleus which shows the characteristics of a “low ionization nuclear emission-line region” (LINER, [7]). LINERs make up a significant fraction of all galaxies (between 1/5 and 1/3; [8]), and because M81 is the nearest LINER it is particularly important for investigating the X–ray emission from such objects.

M81 has been the subject of a number of X–ray studies. It was first observed with *Einstein* [4,5] which resolved several discrete sources, the brightest of which was associated with the active nucleus. An apparently diffuse emission component associated with the bulge of M81, spatially extended over a few arcminutes, was detected first with *ROSAT* [14,9] and confirmed with *Chandra* data [17]. X–ray spectra from *ROSAT* [9], *BBXRT* [12], *ASCA* [10] and *BeppoSAX* [11] suggested the presence of a soft (< 1 keV) thermal component in addition to an absorbed power law component from the nucleus. In this paper we examine the soft X–ray spectrum of M81 at much higher resolution, from an observation with the *XMM-Newton* reflection grating spectrometer (RGS, [6]).

2. RGS data reduction

M81 was observed by *XMM-Newton* on the 22nd and 23rd April 2001 for a total of 138 ks. The RGS data were reduced using the *XMM-Newton* standard analysis software (SAS) public release version 5.2. The source spectrum was extracted from a region centred on the nucleus, enclosing 90% of the point spread function in the cross-dispersion direction, while first and second order selection was performed so as to include 93% of the expected CCD pulse height distribution of the source photons. Background regions were selected in the cross-dispersion direction so as to exclude 99% of the nuclear point spread function; identical order selection was performed on nuclear and background regions. Instrumental features such as the oxygen edge feature near 23 Å were corrected by dividing the effective area calibration in each response matrix by the model/data ratio from a power law fit to the RGS spectrum of the continuum source Mrk 421. First and second order spectra from RGS1 and RGS2 and their corresponding response matrices were resampled to match the RGS1 first order spectrum. They were then combined, and rebinned by a factor of 3 (to ~ 30 mÅ bins) to improve the signal to noise ratio before spectral analysis using XSPEC.

3. The RGS spectrum

Fig. 1 shows the RGS spectrum. The spectrum does not appear to contain the strong absorption lines which characterise AGN warm absorbers (e.g. [1,15]). However, a number of prominent emission lines from H-like and He-like N, O, and Ne as well as L shell lines from Fe XVII and Fe XVIII are visible above the continuum; these are labelled in Fig. 1. The lines are consid-

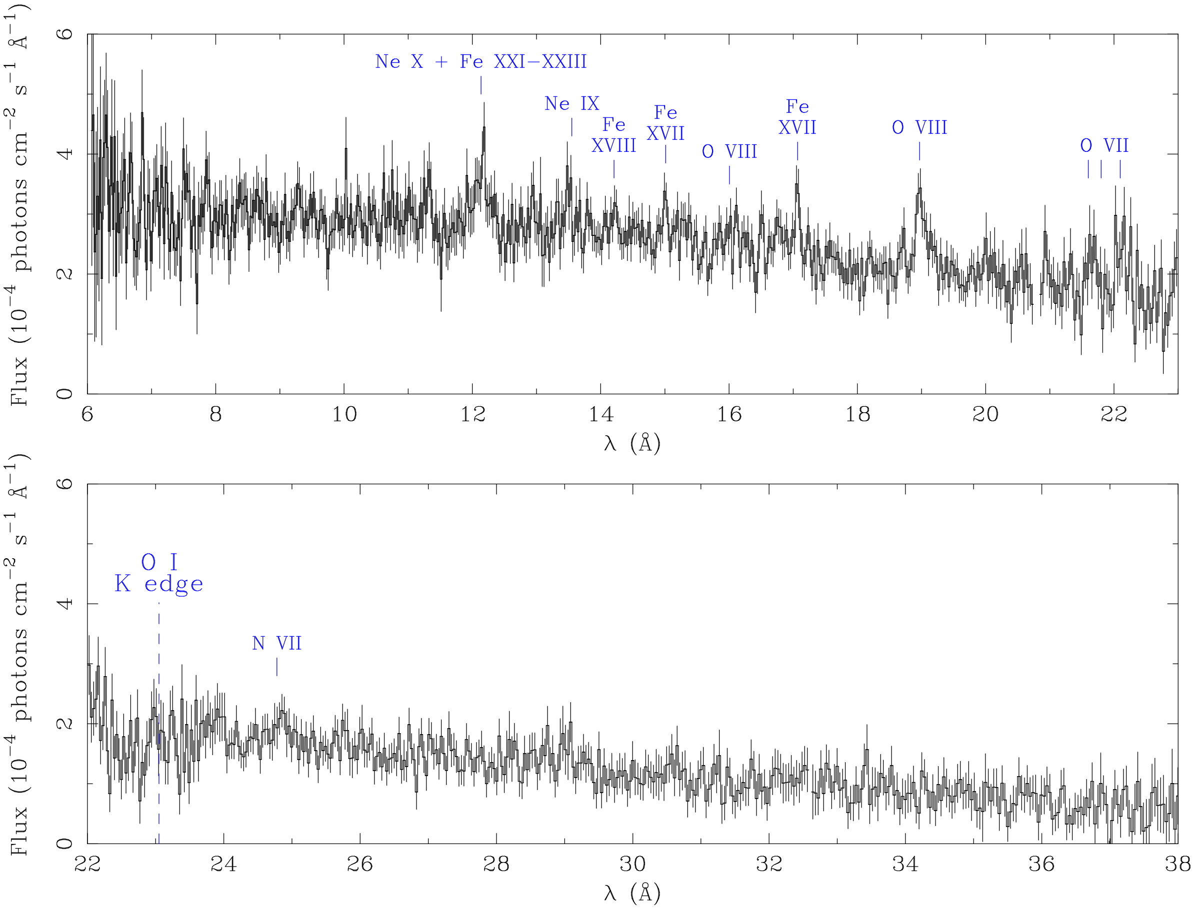

Figure 1. The combined RGS 1+2 spectrum with prominent emission lines marked

erably broader than the RGS line spread function for a point source. For example, O VIII Lyα at $\sim$ 19 Å is expected to have relatively little contamination from neigbouring lines, but a Gaussian fit to this line shows that it is inconsistent with $\sigma = 0$ at $> 99\%$. This broadening could be due to kinematic motions in the gas, for example if it is associated with the active nucleus. However a similar level of line broadening would result from the gas being extended over a region of $\sim$ 2 arcminutes, because the RGS is a slitless dispersive spectrograph and its resolution is degraded for extended objects.

To distinguish between these alternatives, we have examined the spatial distribution of the emission line gas in the RGS cross-dispersion direction by constructing spectra in 40 arc-second wide strips at a range of distances from the nucleus of M81. The spectra were binned to 60 mÅ bins and a background spectrum was constructed from the average of the two strips which are furthest off-axis; this was subtracted from all the spectra. The emission-line rich 14-20 Å parts of these spectra are shown in Fig. 2. The emission line gas, and in particular O VIII Lyα, is extended over more than an arc-minute implying that the excess broadening of the emission lines is due to their spatial extent rather than kinematic motions.

We further investigated the nature of the emission line gas using plasma diagnositics from the He-like O VII triplet, as described in [13]. Taking the 21-23 Å portion of the RGS spectrum, and assuming an underlying power law ($\Gamma = 2$) con-

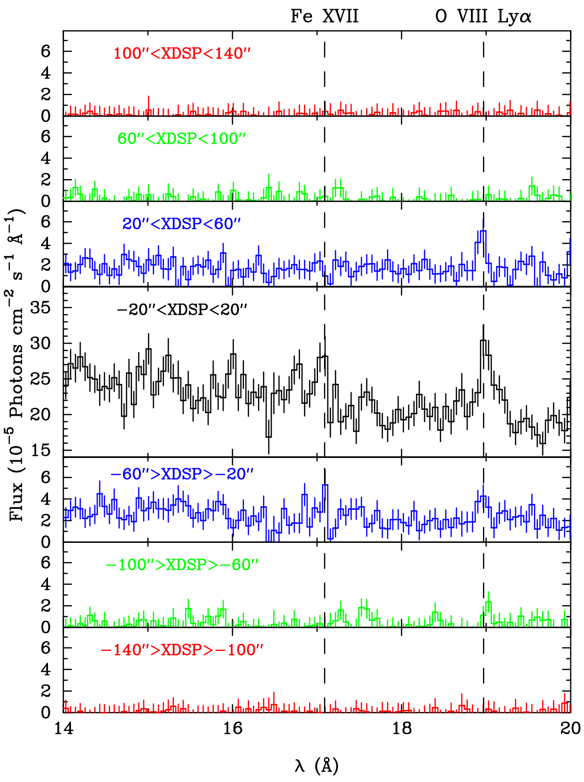

Figure 2. Spectral cuts labeled by distance from the nucleus in the cross-dispersion direction (XDSP).

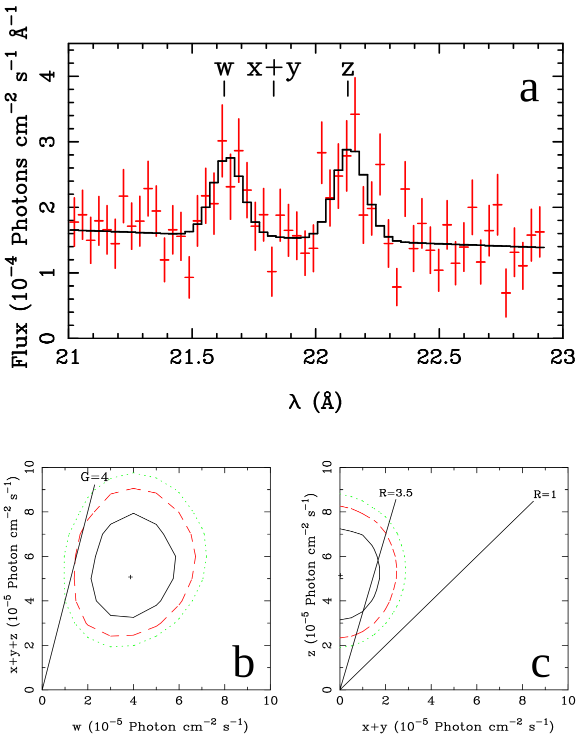

Figure 3. The O VII triplet and best fit model (panel a), confidence contours for intercombination+forbidden line strength against resonance line strength (panel b) and confidence contours for forbidden line strength against intercombination line strength (panel c).

tinuum (see Section 4), we fitted the O VII lines as 3 gaussians with the wavelengths of the resonance (w), intercombination (x+y) and forbidden (z) lines fixed at their theoretical values. The best fit has an acceptable $\chi^2/\nu = 56/51$, and is shown superimposed on the 21-23 Å RGS spectrum in Fig. 3a. In Fig. 3b we show the confidence contour of the (x+y+z) against w line strength, a diagnostic of the ionization mechanism. The solid line shows the line ratio G = (x+y+z)/w = 4. As shown in figure 7 of [13], plasmas in which photoionization is the dominant ionization mechanism are expected to have ratios to the left of this line (i.e. G > 4); this is ruled out at 95% confidence in M81. In plasmas with line ratios to the right of this line, such as that seen in M81, collisional excitation is important and may be the dominant emission mechanism. Fig. 3c shows confidence contours of the density diagnostic z against (x+y). The line shown on the plot corresponding to ratio R = z/(x+y) = 1 is excluded at > 95% along with all of parameter space to the right of this line, implying (see figure 8 of [13]) that the line emitting plasma has a density of $n_e < 10^{11}\mathrm{cm}^{-3}$. The best fit has very weak x+y lines relative to w, and consequently lies to the left of the line R=3.5, hence the line ratio is best reproduced by a low density ($n_e < 10^9\mathrm{cm}^{-3}$) plasma.

4. Modelling the spectrum

It is evident from Fig. 1 that the emission lines in the soft X–ray spectrum of M81 are superimposed on a strong continuum source, almost certainly from the active nucleus at the

Table 1
Spectral fitting of the whole M81 RGS spectrum. All models include Galactic absorption of $N_H = 4.16 \times 10^{20}$cm^{-2}

(1) Model	(2) Γ or kT	(3) flux	(4) N_H	(5) χ^2/ν
PL$\times$N$_H$	2.06 ± 0.06	99.9 ± 3.8	4.8 ± 0.8	1085/992
PL$\times$N$_H$	1.94 ± 0.07	95.8 ± 3.7	3.3 ± 0.8	876/990
+Mek	0.66 ± 0.04	$4.3^{+0.9}_{-0.7}$		
PL$\times$N$_H$	1.93 ± 0.07	94.5 ± 3.8	3.4 ± 0.8	821/984
+Mek3	$0.20^{+0.04}_{-0.02}$	1.5 ± 0.5		
+Mek3	0.66 ± 0.05	$4.2^{+0.8}_{-0.7}$		
PL$\times$N$_H$	1.94 ± 0.06	$91.6^{+7.4}_{-4.4}$	3.4 ± 0.8	803/980
+Mek3	0.18 ± 0.04	$1.1^{+0.5}_{-0.4}$		
+Mek3	0.64 ± 0.04	$4.2^{+0.8}_{-0.9}$		
+Mek3	$1.7^{+2.1}_{-0.5}$	$3.4^{+7.6}_{-2.2}$		

Explanation of columns:
1 PL = power law,
NH = neutral absorber ('tbabs' model in XSPEC),
Mek = thermal plasma ('Mekal' model in XSPEC),
Mek3 = thermal plasma ('Mekal' model in XSPEC) with components shifted by $\pm 0.5\%$ in wavelength to mimic the broadening of the lines produced by the spatial extent of the emission region.
2 power law photon index or temperature of thermal plasma (keV)
3 flux of model component in the energy range 0.3-2.0 keV, in units of 10^{-13} erg cm^{-2} s^{-1} after correction for Galactic absorption of $N_H = 4.16 \times 10^{20}$ cm^{-2}
4 intrinsic neutral column density (cm^{-2}).

heart of M81. Therefore we began by fitting a power law model with absorption (using the xspec model TBabs [19]) due to the line-of-sight Galactic column density, $N_H = 4.16 \times 10^{20}$ cm^{-2}. We found that the power law model is a poor fit with $\chi^2/\nu = 1289/993$; the model overpredicts the data at both the high and low wavelength ends of the spectrum, and has too small an O I edge at 23 Å. We therefore added additional cold absorption, and obtained a much better fit ($\chi^2/\nu = 1085/992$), with an additional $N_H \sim 5 \times 10^{20}$ cm^{-2}. The parameters derived from this fit, and subsequent fits, are given in Table 1. The additional column density confirms that the nucleus of M81 has some intrinsic absorption.

We next attempted to model the emission line component of the spectrum. As shown in Section 3 the O VII triplet is consistent with an origin in a collisionally ionized gas, and the line emission comes from a region extended over several kpc. We therefore began modelling the emission lines by adding a single temperature 'Mekal' thermal plasma model to the absorbed power law model. This resulted in a significant improvement in the fit ($\chi^2/\nu = 876/990$) for a plasma temperature of 0.66 ± 0.04 keV. However, the emission lines are too narrow in this model (the excessive width of the emission lines has already been pointed out in Section 3), and some emission lines, most noticeably those from O VII, have much lower intensities in the model than in the observed spectrum. We therefore added a second, lower temperature, Mekal component to the model, and at both Mekal temperatures we added components shifted by $\pm 0.5\%$ in wavelength to broaden the line profiles. This resulted in another significant improvement in χ^2, reproducing most of the emission lines well, with the second plasma component at a best fit temperature of ~ 0.2 keV. However, the blend of Ne X with Fe XXII-XXIII at ~ 12.1 Å is still underproduced by this model, and so a third, higher temperature, broadened Mekal plasma was added. This resulted in yet another significant improvement in the fit, to a final $\chi^2/\nu = 803/980$, with a best fit temperature for the third Mekal component of $1.7^{+2.1}_{-0.5}$ keV. The model reproduces the spectrum well, as shown in Fig.4.

5. Discussion

In Section 3 we showed that the soft X–ray emission lines in M81 come from a region which is extended in both the dispersion direction (evidenced by the excess width of the lines) and cross-dispersion direction (see Fig.2) of the RGS. Absorption lines, characteristic of AGN warm absorbers, are not apparent in the RGS spectrum of M81. The diagnostic O VII triplet is emitted by a low density region and appears to be collisionally ionized rather than photoionized by the central AGN. Furthermore, a 3 temperature thermal plasma model provides a good description of the emission line component of the M81 RGS spectrum, in conjunction with powerlaw emission from the nucleus which is subject to some absorption by cold material. Two of the plasma components have well constrained temperatures of 0.18 ± 0.04 keV and 0.64 ± 0.04 keV, which are characteristic of the hot interstellar medium produced by supernova explosions; in this case we would expect these emission lines to come from a genuinely diffuse region (or regions) in the bulge of M81.

X-ray imaging studies, first using *ROSAT* [14, 9], and later using *Chandra* [17] have indeed found apparently diffuse emission associated with the bulge of M81. Immler & Wang [9] extracted a PSPC spectrum of the M81 bulge using a 1 arcmin radius source circle, including both the active nuclues and the diffuse emission. They found a good fit using an absorbed power law to represent the nucleus and a two-temperature thermal plasma to represent the diffuse emission. The best fit temperatures of the plasma, 0.15 ± 0.02 keV and 0.63 ± 0.11 keV, are in extremely good agreement with the temperatures obtained from the RGS spectrum. However the spatial resolution of *ROSAT* (~ 5 arcsec for the HRI and ~ 20 arcsec for the PSPC) was such that the emission from a large population of weak point sources could easily be confused with genuinely diffuse emisson.

The much higher resolution observation performed with *Chandra* provides a much more accurate determination of the truly diffuse emission from the nucleus. Tennant *et al.* [17] found that of the bulge emission, even excluding the nucleus, 64% comes from the resolved point source population. The remaining unresolved bulge emission has a countrate of 0.092 s^{-1} in the *Chandra* ACIS-S3 chip. The 0.18 keV and 0.64 keV thermal plasma components from our best fit model in Table 1 would correspond to countrates of 0.036 s^{-1} and 0.158 s^{-1} in the same chip. The lowest temperature component alone is unable to account for all the unresolved bulge emission, but the combinaton of the two exceeds it.

This implies that some of the emission associated with the 0.64 keV thermal plasma, and all of the emisson associated with the highest of the three plasma temperatures ($1.7^{+2.1}_{-0.5}$ keV) must arise in part of the bulge population resolved by *Chandra*. There are no massive, young stars in the bulge of M81 [2]. We therefore propose low-mass X–ray binaries as the most likely origin of this higher temperature emission.

If the diffuse X-ray emitting gas is sustained by supernovae, we can use the simulations of Shelton [16] to estimate the approximate required supernova rate. The combined flux from the 0.18 keV and half the 0.64 keV thermal plasma components corresponds to supernova rates of between $\sim 4 \times 10^{-3}$ year^{-1} and $\sim 2 \times 10^{-2}$ year^{-1}. As there are no young stars in the bulge of M81 the supernovae would have to be type Ia. The canonical 'expected' rate for type Ia supernovae in M81 from table 8 of Van den Bergh & Tammann [18] is $\sim 6 \times 10^{-3}$ year^{-1}, consistent with the rate of supernovae required to support the diffuse X-ray emission.

If the diffuse X-ray emission is indeed produced by supernova remnants, then fast shocks must be propagating through the bulge, and this could explain the optical line emission which gives M81 its LINER classification.

For example, the [O III]/Hβ ratio in the bulge of M81 is similar to the predictions of the shock model of Dopita & Sutherland ([3]) for shock velocities of 300 km s^{-1}. In this model, [O III] λ5007

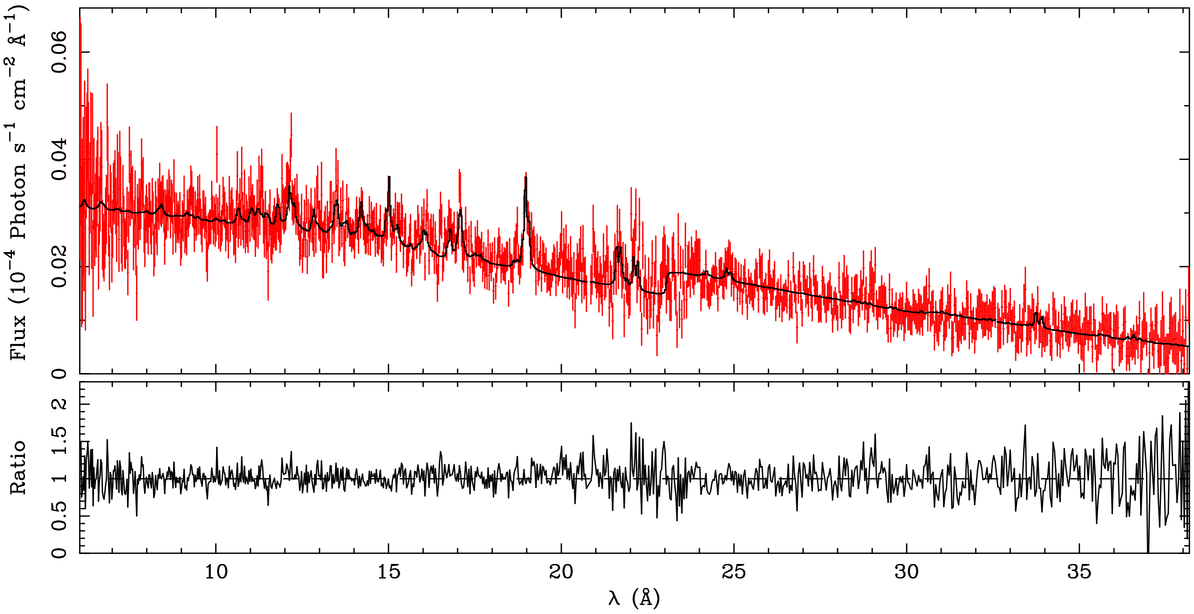

Figure 4. Power law + intrinsic neutral absorption + 3 Mekal model fit to the RGS spectrum

is emitted by gas which is photoionized by the shock-heated material, and for a shock velocity of 300 km s^{-1} the shocked material has an electron temperature similar to the 0.2 keV plasma found in the RGS spectrum. This suggests that the optical line-emission is related to the soft X-ray line-emitting plasma, and that the interstellar medium in the bulge of M81 is shock-heated, possibly by supernovae.

REFERENCES

1. Blustin A.J., Branduardi-Raymont G., Behar E., *et al.* , 2002, A&A, 392, 453
2. Devereux N., Ford H., Jacoby G., 1997, ApJ, 481, L71
3. Dopita M.A., Sutherland R.S., 1995, ApJ, 455, 468
4. Elvis M., van Speybroeck L., 1982, ApJ, 257, L51
5. Fabbiano G., 1988, ApJ, 325, 544
6. den Herder J.W., Brinkman A.C., Kahn S.M., *et al.* , 2001, A&A, 365, L7
7. Heckman T.M., 1980, A&A, 87, 152
8. Ho L.C., Filippenko A.V., Sargent W.L.W., 1997, ApJ, 487, 568
9. Immler S., Wang Q.D., 2001, ApJ, 554, 202
10. Ishisaki Y., Makishima K., Iyomoto N., *et al.* , 1996, PASJ, 48, 237
11. Pellegrini S., Cappi M., Bassani L., Malaguti G., Palumbo G.G.C., Persic M., 2000, A&A, 353, 447
12. Petre R., Mushotzky R.F., Serlemitsos P.J., Jahoda K., Marshall F.E., 1993, ApJ, 418, 644
13. Pourquet D., Dubau J., 2000, A&A Supp, 143, 495
14. Roberts T.P., Warwick R.S., 2000, MNRAS 315, 98
15. Sako M., Kahn S.M., Behar E., *et al.* , 2001, A&A, 365, L168
16. Shelton R.L., 1998, ApJ, 504, 785
17. Tennant A.F., Wu K., Ghosh K.K., Kolodziejczak J.J., Schwartz D.A., 2001, ApJ, 549, L43
18. van den Bergh S., Tammann G.A., 1991, Annu. Rev. Astron. Astrophys., 29, 363
19. Wilms J., Allen A., McCray R., 2000, ApJ, 542, 914

ACKNOWLEDGEMENTS

Based on observations obtained with *XMM-Newton*, an ESA science mission with instruments and contributions directly funded by ESA Member States and the USA (NASA).